Development of a visualization tool for PIC simulations of plasma acceleration

Andrea Mauri, FLA

September 8th, 2011

Abstract

This review contains an overview on Laser Plasma Acceleration, dealing with the basic principle of laser-plasma interaction and one of the algorithm developed to simulate the motion of huge number of electrons in their selves-consinstence electro-magnetic fields inside an underdense plasma. Then we will focus on the development of a Matlab tool to visualize RAW simulation files, in this report we present some plots concerning external bunch injections that could be on axis with the laser pulse or with a transverse offset usefull to investigate electron beam properties and the electic field inside plasma.

Contents

1 Introduction

The concept of plasma acceleration utilizes high-intensity laser pulses or particle beams for the excitation of extreme charge-density modulations in plasmas. These modulations may support field gradients of more than 100 GV/m and propagate as waves through the plasma medium with velocities close to the speed of light. Thus, they are suited perfectly for the acceleration of copropagating, charged particle beams.
Nowadays, ultra-short electron-packets of only few-micrometer length consisting of up to 10^9 particles are routinely driven to energies of more than one GeV when using this process over distances on a centimeter scale. Owing to the fact that plasmas allow a thousandfold increase in electric field strength compared to modern accelerating structures of conventional design, they raise hopes for a revolution and miniaturization of todays particle-accelerator technology.
In addition, plasma-generated, ultra-relativistic electron beams are intrinsically short and therefore constitute potentially attractive drivers for radiation sources of highest brilliance. [1]

2 Fundamental of Plasma Acceleration

Structured systems in nature have binding energies larger than the ambient thermal energy, but when placed in a sufficienly hot environment they decompose. At temperatures near or exceeding atomic ionization energies, atoms decompose into negativly charged electrons and positively charged ions. These charged particles aren't free but they are strongly affected by each others' electromagnetic fields and their assemblage becomes capable of collective motions: such an assemblage is termed a *plasma* if it is quasi-neutral in time and space (see below).
In the particular case of laser wakefield accelaration the ionization process is due to the high photon flux or to the strong laser field.

2.1 Basic plasma properties

Plasmas macroscopically contain equal numbers of positive and negative charge carriers, so that the oppositely charges electrically neutralize one another on macroscopic length-scales. This plasma propertiy is called quasi-neutrality.
Quasi-neutrality condition demands that

$$Zn_i \simeq n_e \tag{1}$$

where Z is the degree of ionization.
The length-scale that over which the quasi-neutrality condition is realized is given by the Debye length

$$\lambda_D = \sqrt{\frac{\varepsilon_0 \, k_B T_e}{n_e \, e^2}}. \tag{2}$$

where k_B is Boltzmanns constant, n_e and T_e are the electron density and temperature, respectively. Note that λ_D is independent on electron mass.
The Debye length is directly connected to another important quantity, the plasma parameter:

$$\Lambda = \frac{4\pi}{3} n_s \lambda_D^3 \tag{3}$$

which represents the number of particles of species s and of density n_s located within a sphere of radius λ_D (Debye sphere). [2]

On scale lengths smaller than λ_D there is no electric screening effect and hence, an infinitesimal charge separation give rise to plasmsa oscillations at a well defined *electron plasma frequency*, given by the following form:

$$\omega_P^2 = \frac{n_e e^2}{\varepsilon_0 m_e} \tag{4}$$

Figure 1 and 2 show the values of debye length and plasma frequency as functions of the electron density.

2.2 Laser propagation in plasma

An important parameter in the discussion of intense laser-plasma interactions is the laser strength parameter a_0, defined as the peak amplitude of the normalized vector potential of the laser field $\mathbf{a} = e\mathbf{A}/m_e c^2$.
In Laser Wake Field Acceleration (LWFA) plasma waves are driven by the laser pulse via the ponderomotive force. The ponderomotive force can be derived by considering the electron fluid momentum equation in the cold fluid limit,

$$d\mathbf{p}/dt = -e[\mathbf{E} + (\mathbf{v} \times \mathbf{B})/c], \tag{5}$$

where $\mathbf{p}$ and $\mathbf{v}$ are the plasma fluid element momentum and velocity respectiely. Writing the electric and magnetic fields as $\mathbf{E} = -\partial\mathbf{A}/\partial ct$ and $\mathbf{B} = \nabla \times \mathbf{A}$ the expression for the ponderomotive force in the linear limit becomes

$$\mathbf{F}_p = m_e c^2 \nabla(\mathbf{a}^2/2) \tag{6}$$

In the linear regime ($\mathbf{a} \ll 1$) waves excited by the laser into the plasma propagate linearly and electron density and electromagnetic field exhibit sinusoidal shapes.
For $\mathbf{a}$ on the order of or larger than 1 plasma waves becomes highly nonlinear and electron density becomes strongly peaked (as shown in figure 3). Consequently the electric field shows a non linear sawtooth profile that has a high magnitude, which is used to accelerate electrons which can be externally injected by a pre-accelerated beam or intrinsically injected from the plasma. Due to nonlinear effects the wave length increases as the amplitude increases. [1]

[1] Bulanov *et al.*, 1989; Berezhiani and Murusidze, 1990; Sprangle *et al.*, 1990.

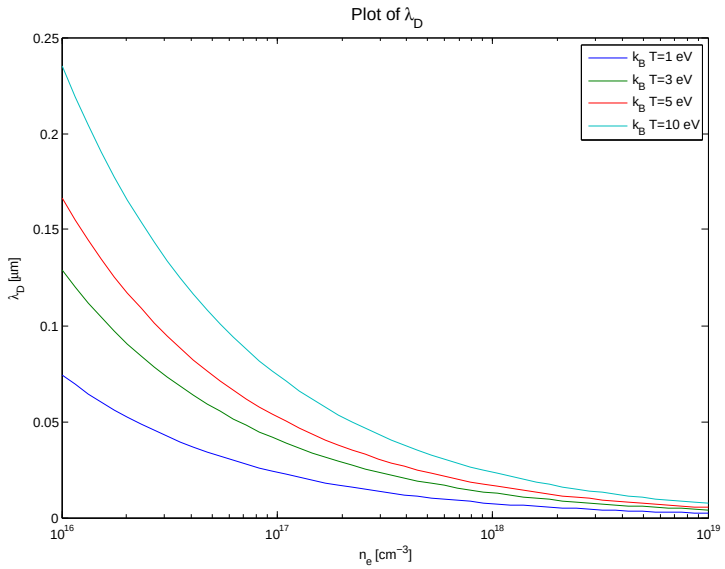

Figure 1: Debye length, function of electron density at different plasma temperature.

The phase of the plasma wave that is capable of accelerating negatively charged particles is depicted in figure 3 as the area for which the longitudinal electric field is negative. This phase increases with increasing nonlinearity of the plasma oscillation and the longitudinal electric field then has a linear dependence on the co-moving variable ξ.

Depending on the relative speed between plasma waves and electrons, the accelerated bunch moves forward or backward with respect to the electric field propagated in the plasma-wave. Generally, the plasma phase velocity is equal to the laser group velocity, which can be obtained from the laser pulse frequency $\omega^2 = c^2k^2 + \omega_P^2$, that yields [2] [4]

[2]Nonlinear corrections have been analized by Decker and Mori (1994) and Esarey *et al. (2000)*

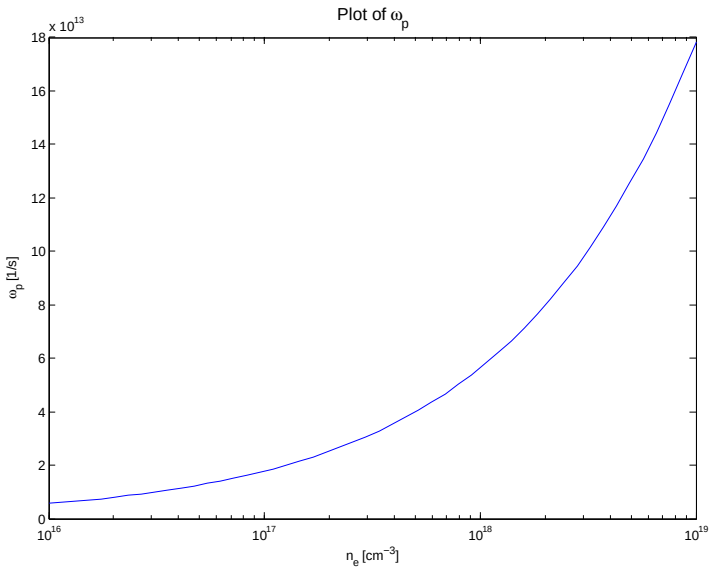

Figure 2: Plasma frequency in function of the electron density.

$$v_g \simeq c(1 - \omega_P^2/\omega^2)^{1/2} \tag{7}$$

and

$$\gamma_g \simeq (1 - v_g^2/c^2)^{-1/2} = \omega/\omega_P. \tag{8}$$

Experiments with externally injected electron bunches at REGAE facility, DESY, will use underdense plasma (with an electron density on the order of $n_e = 0.1 \cdot 10^{18}$ cm^{-3}), which gives $\gamma_g \simeq 120$, to compare with the electron bunch gamma factor $\gamma = 5MeV/m_e \simeq 10$.

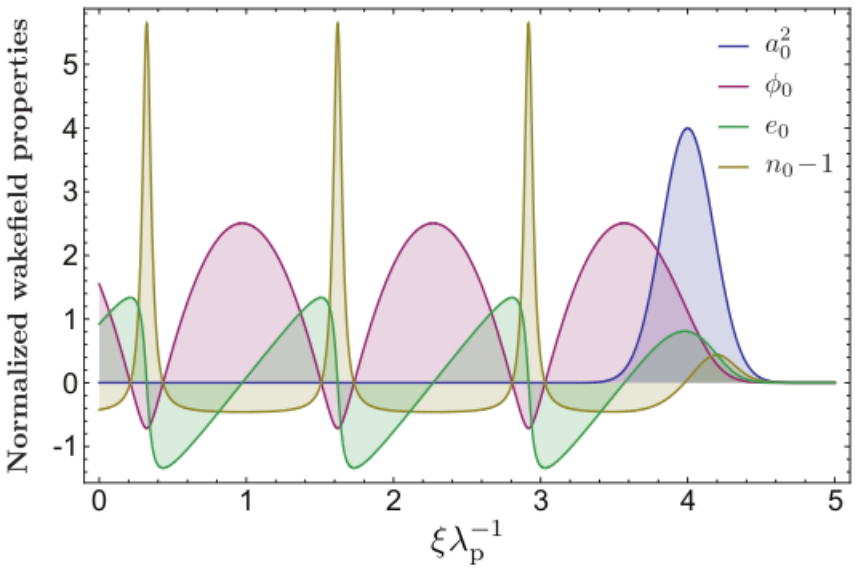

Figure 3: The properties of a wakefield generated by a Gaussian shaped laser pulse with $\mathbf{a} = 2$. We can see the laser shape (blue), the electron density (yellow) and the consequent electric field (green). All spatial scales are normalized to the non-relativistic plasma wavelength λ_P and ξ represents the co-moving variable defined as $\xi = z - ct$. [3]

This means that the electron bunch moves backwards in the wakefield and such a movement make the bunch thinner during the acceleration process due to higher values of the electric field that acts on the backside bunch particles.

(9)

3 PIC simulation

Laser-driven wakefield generation and electron acceleration in a tenuous plasma can generally not be treated by analytic theory owing to a highly nonlinear electron motion at relativistic intensities and the complicated interplay between high intensity laser pulses and large amplitude plasma wakes. Therefore, only numerical simulations provide means for virtually full-featured and instructive theoretical investigations.
Because of the huge number of particles in laboratory and natural plasmas, it is impossible for computer simulation to compute the motion of each single particle in their self-consistent electric and magnetic fields. To solve this problem some models for computer simulation have been developed, one of the most succesfull algorithm is the particle-in-cell (PIC) code, which consists in considering each particle in the simulation as representing many particles of real plasma (a macroparticle). This allow us to reduce the

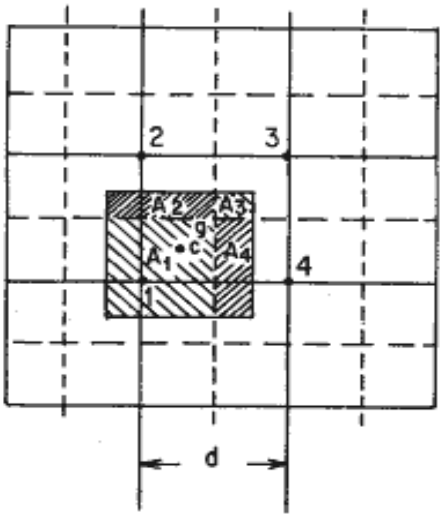

Figure 4: Area-weighting method for charge sharing in two dimensions. [5]

numer of particle of a factor between 10^3 and 10^5 and consequently the requirements for computational power. Furthermore in PIC simulations, the electromagnetic field is discretized on a spatial grid, whereas particles have continuous positons and momenta.

Current deposition approximation In one of the most common procedure to discretized field and particles current we need to consider a two dimensional or three dimensional grid and distribute weighted particles charge and current at the nearest grid points (four, in the two dimensional case), as shown in figure 4, such that the total charge and dipole moment with respect to the center of the cell are the same.
The heavy lines show the main computational grid, grid spacing d; the dashed lines show a grid whose grid points lie at the centers of the squares of the main grid. Consider a particle whose center is at pooint C. Take this to be the center point of a square with size d, equal to the grid spacing. The intersection of this square with the dashed grid divides this square into four areas, A_1, A_2, A_3, A_4, as shown in the figure. Assign to grid point 1 a charge $qA_1/d2$ and to grid points 2,3 and 4, charges $qA_2/d2$, $qA_3/d2$ and $qA_4/d2$, respectively.
One can readily verify that this distribution of charge has the same dipole moment with respect to the nearest dashed grid point g as the original particle has. This simple interpolation scheme can be easily extended to three dimensions. [5]

The working principle of PIC codes may briefly be summarized in the following way (and shown in figure 5). Starting from initial macroparticle distributions and currents, and

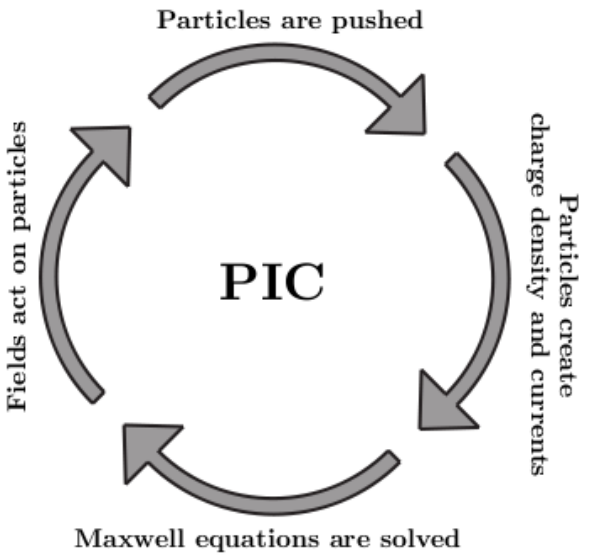

Figure 5: A simple particle-in-cell algorithm calculation cycle. [3]

from discrete, initial conditions representing the state of the electro-magnetic fields on the grid, Maxwells equations are solved. Thus, the field grid is modified and subsequently acts on the particles. Consequently each particle is moved inside the simulation volume according to the calculated solution of its equation of motion driven by the electro-magnetic grid potentials. The generated particle streams represent currents and set up new charge-density distributions. This again requires the solution of Maxwells equations and initiates the next calculation cycle. [3]

4 Visualization of simulations

In all the fields of physics it is fundamental to compare theory and experiments. Here we want to study the plasma behaviour in order to understand which are the best values and conditions to take in the realization of the experimental device.
We need to elaborate a huge number of data (each simulation file contains more then 300,000 macroparticles and for all of them specifies the spatial position in 1, 2 or 3 dimensions, the momentum and the weighted charge) and we used MATLAB as a powerfull tool to visualize the risults of our simulations. [6]
Analizing the final shape, divergence, energy of the bunch we can understand how far are we from what we want to achieve, in our case a stable ultra-relativistic electron beam, we can also probe the fields in the acceleration process.
Figure 6 show an example of final visualization of a simulation run by the FLA plasma group.

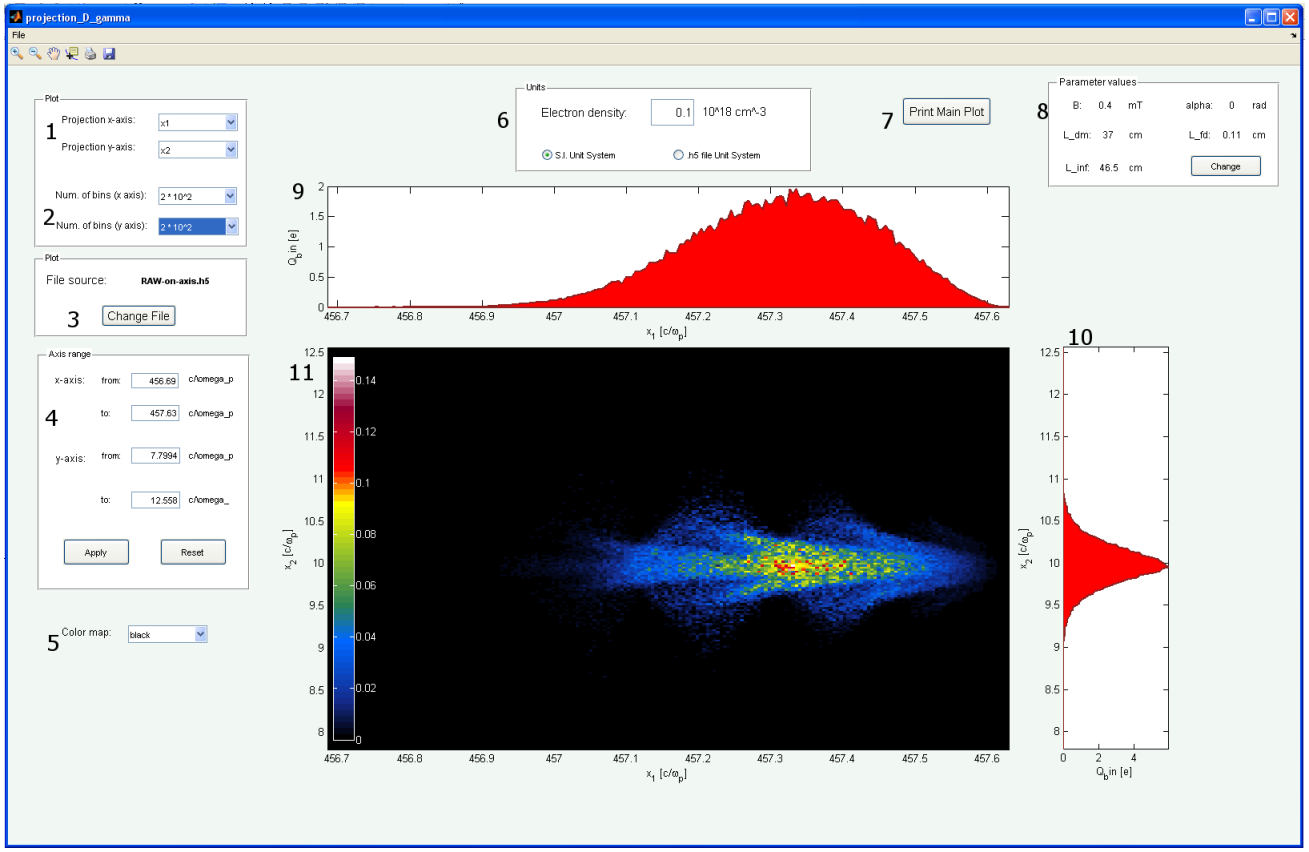

Figure 6: Example of the final Matlab interface. 1: selection of the quantities to visualize; 2: resolution, number of bins to divide the range between the highest and the lowest values of the selected variables; 3: source simulation file; 4: range of values to plot, the default selection is between the minimum and the maximum; 5: choise of the colormap, the intensity scale of colour for the main plot; 6: swicth between the normalized unit and the SI unit, that require to specify the electron density; 7: button to visualize and print the main plot; 8: parameters of the magnetic permanent dipole device (section 4.2); 9: 2D histogram of the x-axis projection; 10: 2D histogram of the y-axis projection; 11: main plot.

4.1 Comparison between two injection cases

In this subsection we want to discuss what happens if the pre-accelerated buch is injected on the laser axis or with a transverse offset.
Figure 7 and 8 show the trasversal phase space and the final bunch shape respectively for on axis injection and out of axis injection. In this second case the initial offset was 0.5 σ_{x_2} .
In the simulation of off-axis injection, the particles of the final bunch have different phases (as results from ring in the phase space of figure 8) due to the variable strength of electromagnetic field in time and space. In fact the distribution on the longitudinal plane show oscillations in the x_2 axis.
On the other hand, on the on axis injection, this speading phase effect produce just a modulation of the shape of the electron beam (figure 7).

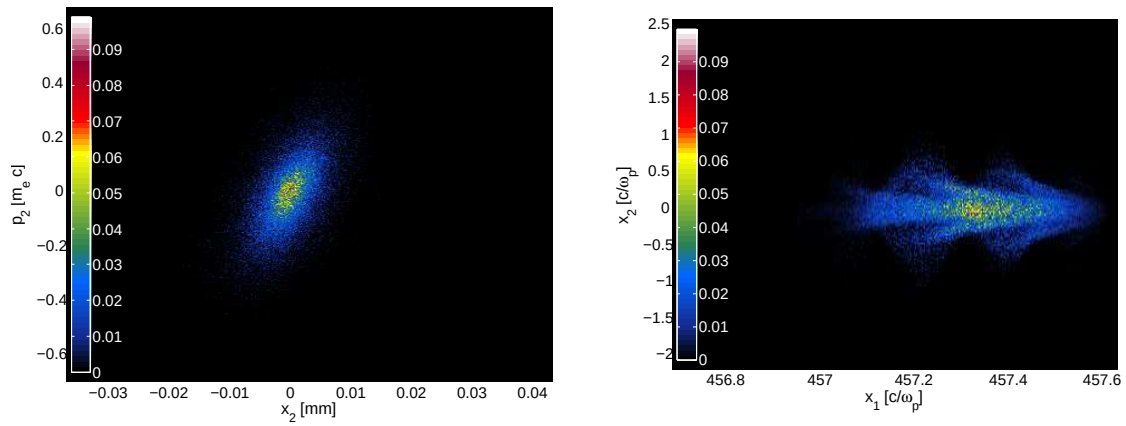

Figure 7: External injection on axis: trasversal phase space (left); section of the bunch in the longitudinal plane (right)

4.2 Divergence and energy beam diagnostic

A characterization of the accelerated electron bunches was conducted using two different techniques. The beam pointing and divergence was assessed with the help of a scintillating phosphor screen situated directly at the end of the accelerating cavity, this screen

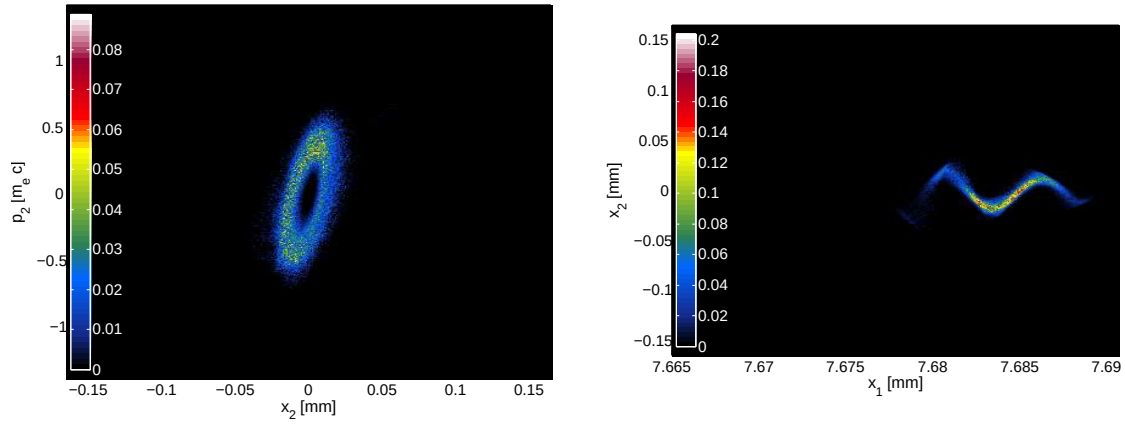

Figure 8: External injection with transerse offset of 0.5 σ: trasversal phase space (left); section of the bunch in the longitudinal plane (right)

could be retracted from the electron-beam path in order to allow for an undisturbed electron bunch propagation. To examine the energy electron distribution, a permanent dipole magnet is placed on the elctron path in order to disperse electrons of different energies and to sent them onto a second charge-calibrated phosphorescence film (figure 9). [3]
Owing to geometrical restrictions, only energies exceeding a certain threshold were captured, in fact particles with energy under such a minimum value can't reach the screen. After traveling through the dipole magnet, the path deviation D of a single electron, which is detected on a screen tilted by an angle α around a pivot point at distance l_{inf} behind the spectrometer, can be written as

$$D(\gamma) = \frac{1}{\cos\alpha}\left[l_z(\gamma)\left.\frac{\partial H(\gamma)}{\partial l_{\mathrm{sp}}}\right|_{l_{\mathrm{dm}}} + H(\gamma)|_{l_{\mathrm{dm}}}\right] \tag{10}$$

Where l_{sp} and l_z denote respectively the distance from the particle position to the magnet-entrance or exit plane. In particular l_z is given by

$$l_z(\gamma) = \frac{l_{\mathrm{inf}} - \tan(\alpha)H(\gamma)|_{l_{\mathrm{dm}}}}{1 + \tan(\alpha)\left.\frac{\partial H(\gamma)}{\partial l_{\mathrm{sp}}}\right|_{l_{\mathrm{dm}}}} \tag{11}$$

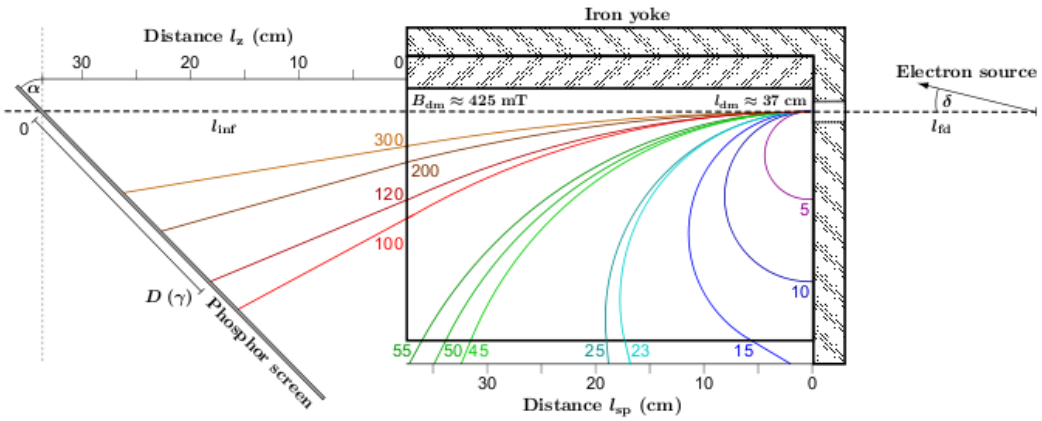

Figure 9: Design of the permanent dipole magnet spectrometer and resulting electron paths. The colored numbers constitute the electron energy in MeV corresponding to an equivalently colored trajectory. [3]

and the electron path deviation H inside the magnet is

$$H(\gamma) = \frac{\gamma m_e c}{eB_{\rm dm}}\sqrt{1-\gamma^{-2}}\left[\cos\left(\arcsin\left[\frac{eB_{\rm dm}}{\gamma m_e c}\frac{l_{\rm sp}}{\sqrt{1-\gamma^{-2}}} - \sin\delta\right] - 2\delta\right) - \cos\delta\right] + \\ + l_{\rm fd}\tan\delta + x_{\rm off} \tag{12}$$

where $l_{\rm fd}$ is the distance from the source of the bunch to the spectrometer entrance, δ is the angle between the electron direction in the trasversal plane and the x axis, and $x_{\rm off}$ is the offset relative to the center of the electron beam.
In order to explore beam properties in both the transverse axis x and y it is sufficient a rotation of 90° of the magnetic field. In the case of an horizontal magnetic field (producing a vertical bending effect), dealing with 2D simulations the transverse offset is imposed to be zero.
Figure 10 show the beam divergence detected thanks to a scintillator screen located at the end of the acceleration path.
Plotting the distance $D(\gamma)$ in function of the energy we can obtain the resolution with which we can measure the electron energy with our spectrometer. Figure 11 shows the function $D(\gamma)$ for the magnetic field value equal to 150 mT. The higher the magnetic field is, the greater the slope of the line is and, consequently, the better the resolution is. Note that the size of the screen is fixed (in our case it is 55cm x 12cm) and for too strong magnetic field electrons can't reach the screen.
We can see how the line describing the function $D(\gamma)$ is thinner for high values of energy and thicker for low energy electrons when divergence and offset contribution increases.
Figure 12 show the detection on the screen for different values of the magnetic field in the case of the external injection with a transverse offset, S2 and D3 are the horizontal

and vertical lengths of the screen respectectively. We can see how, increasing the the magnetic field, we can separate more and more the particles on the screen as predicted. Due to the transverse oscillation of the beam inside the plasma (figure 8), also the electrons detection on the screen presents the same wave motion; for low magnetic field values we can detect just two higher electron density areas, because the bending power is not strength enough to separate the different energetic electrons, increasing the value of the magnetic field we can measure the energy of the bunch.
Comparing the shape of the four different plots in figure 12 we can suppose that the best resolution is obtained by B=150 mT. In fact its shape is really similar to energy distridution (shown in figure 13), the only difference is the contribution due to the divergency and offset of the accelerated beam.

5 Conclusion

As a cutting-edge accelerating technique Laser Plasma Acceleration has still many goal to achieve and, of course, also some limitations, like the depletion of laser pulse or the current technical difficulty of staging, because of the material space that high intensity laser requires to be focused on the gas cavity that conflicts with the necessity of placing the accelerating device really close to the next one to limit the beam divergence.
We understood to visualize and analize the theoretical simulation of plasma wake-field acceleration which is a fundamental step before the realization of experiments. The software I developed with Matlab allow us to convert huge quantity of data in much more physically understandable plots and to investigate the accelerated bunch and fields inside plasma properties.

Aknowledgment

I really would like to thank my supervisors Jens Osterhoff, Timon Mehrling and Julia Grebenyuk and all the members of the Desy Plasma Group for the help they gave me, the patience with which they followed my work here and, expecially, the opporunity they gave me to join their researce group and live this exciting experience.
I also have to thank the Summer Student Program organizers that made this great opportunity possible and made all their efforts to be sure that we enjoyed the project. Thanks expecially to Olaf Behnke for all the ideas and suggestions he gave us to enjoy our stay in Hamburg.

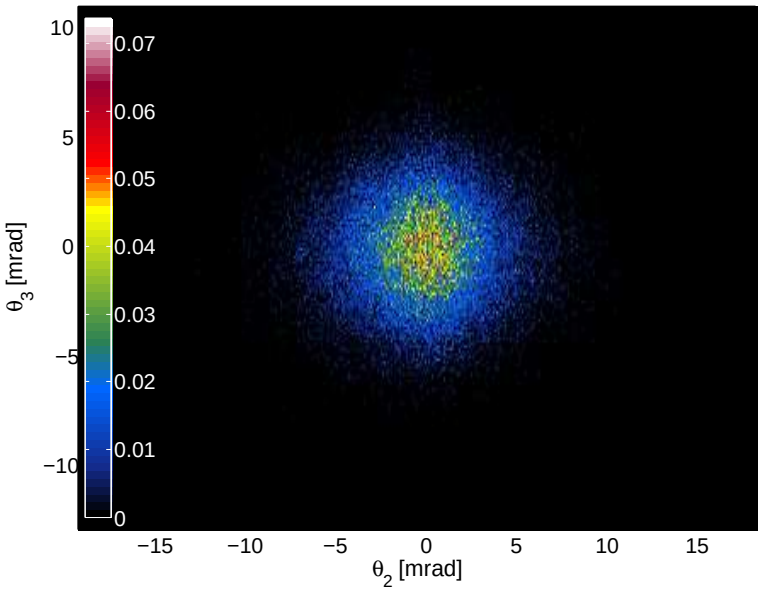

Figure 10: Divergence of an on-axis accelerated electron bunch.

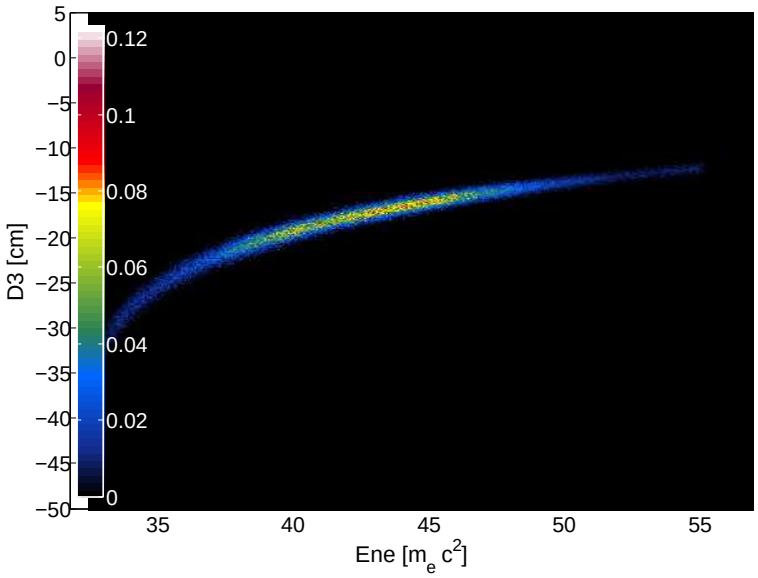

Figure 11: Resoluton of D in function of energy in the case of an horizontal magnetic field of 150 mT.

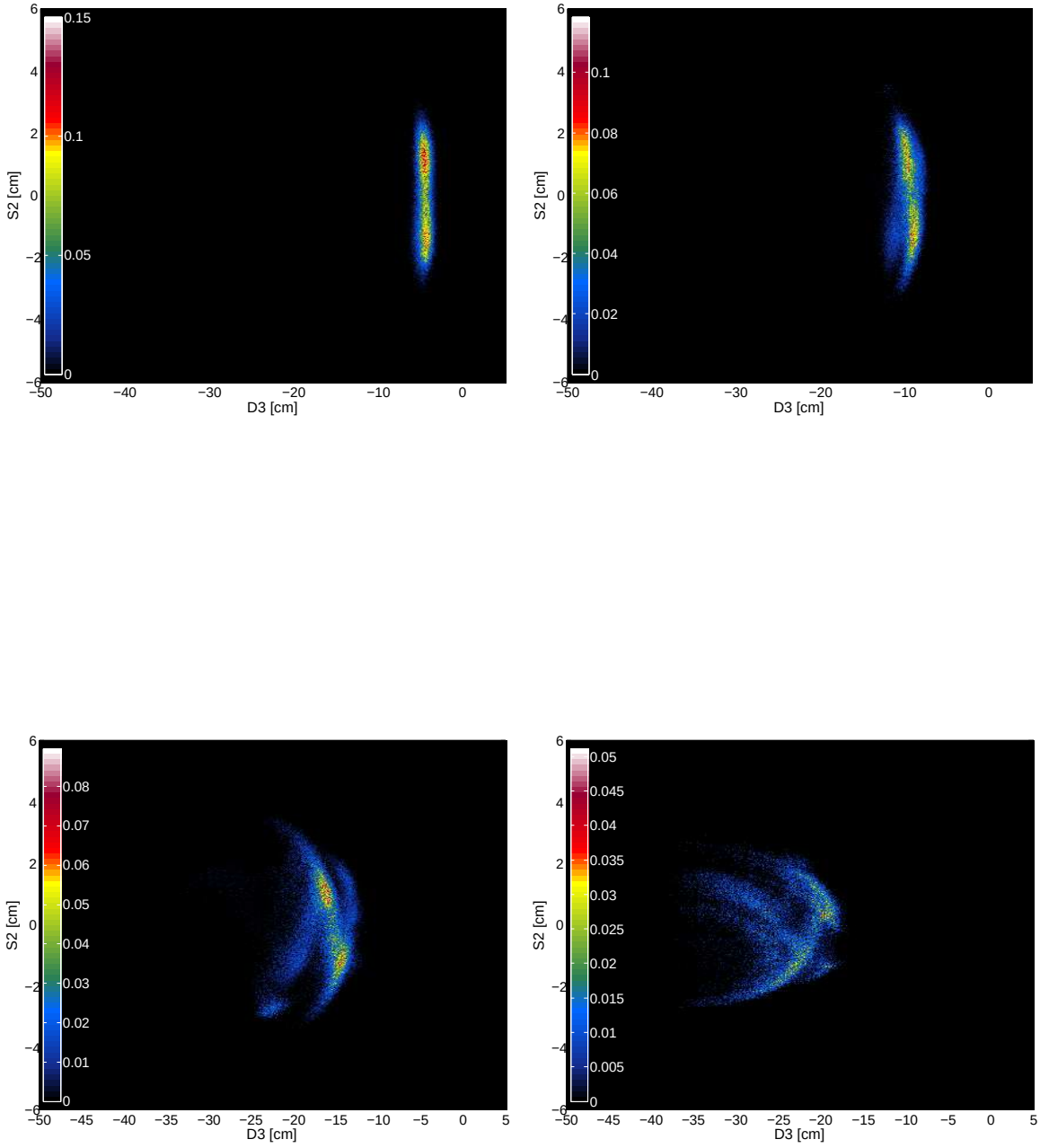

Figure 12: Detection of the electron beam on the scintillating screen after the bending effect of the magnetic field for differen values of the magnetic field, from left to right, B=50 mT, B=100 mT (up) and B=150 mT, B=200 mT (down). The parameter values introduced in figure 9 are set as follow: $l_{dm} = 37$ cm, $l_{inf} = 46.5$ cm, $\alpha = 0$, $l_{fd} = 1$ m.

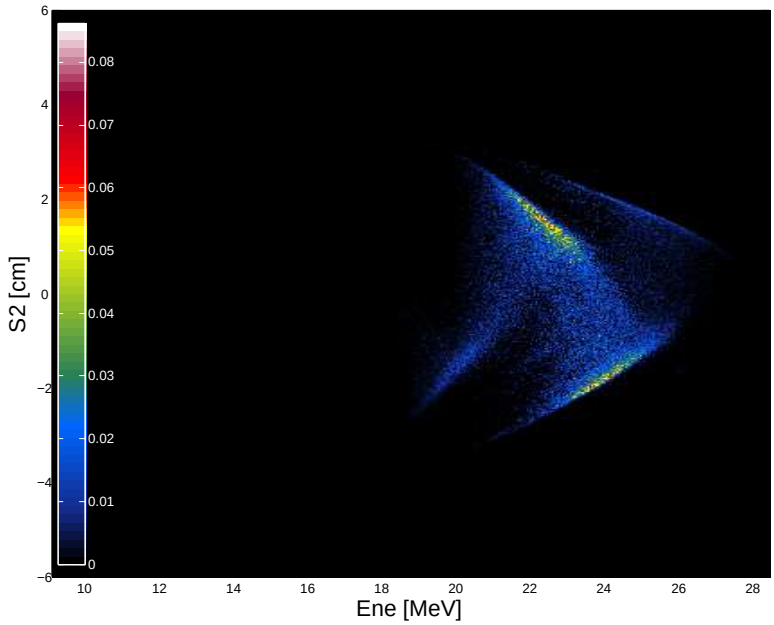

Figure 13: Transversal distribution of the energy of the beam in the case of trasverse offset equals to 0.5 σ and B=150 mT. All the other parameters are set as in figure 12.

References

[1] Desy plasma group web page, *http://plasma.desy.de*

[2] Plasma physics, *Richard Fitzpatrick*

[3] Stable, ultra-relativistic electron beams by laser-wakefield acceleration, *Jens Osterhoff*

[4] Physics of laser-driven plasma-based electron accelerators, *E. Esarey, C. B. Schroeder and W. P. Leemans*

[5] Particle simulation of plasmas, *John M. Dawson*

[6] MATLAB online guide *http://www.mathworks.de/products/matlab/index.html*